*Flow, Turbulence and Combustion* **72:** 333–347, 2004.



# Simulations of Three-Dimensional Turbulent Mixing for Schmidt Numbers of the Order 1000

P.K. YEUNG[1], S. XU[1], D.A. DONZIS[1] and K.R. SREENIVASAN[2]
[1]*School of Aerospace Engineering, Georgia Institute of Technology, Atlanta, Georgia, USA; E-mail: yeung@peach.ae.gatech.edu*
[2]*International Center for Theoretical Physics, Strada Costiera, Trieste, Italy*

Received 10 June 2003; accepted in revised form 14 December 2003

**Abstract.** We report basic results from new numerical simulations of passive scalar mixing at Schmidt numbers ($Sc$) of the order of 1000 in isotropic turbulence. The required high grid-resolution is made possible by simulating turbulence at very low Reynolds numbers, which nevertheless possesses universality in dissipative scales of motion. The results obtained are qualitatively consistent with those based on another study (Yeung et al., *Phys. Fluids* **14** (2002) 4178–4191) with a less extended Schmidt number range and a higher Reynolds number. In the stationary state maintained by a uniform mean scalar gradient, the scalar variance increases slightly with $Sc$ but scalar dissipation is nearly constant. As the Schmidt number increases, there is an increasing trend towards $k^{-1}$ scaling predicted by Batchelor (Batchelor, *J. Fluid Mech.* **5** (1959) 113–133) for the viscous-convective range of the scalar spectrum; the scalar gradient skewness approaches zero; and the intermittency measured by the scalar gradient flatness approaches its asymptotic state. However, the value of $Sc$ needed for the asymptotic behavior to emerge appears to increase with decreasing Reynolds number of the turbulence. In the viscous-diffusive range, the scalar spectrum is in better agreement with Kraichnan's (Kraichnan., *Phys. Fluids* **11** (1968) 945–953) result than with Batchelor's.

**Key words:** turbulence, mixing, passive scalars, schmidt number, numerical simulation, scaling

## 1. Introduction

In applications, turbulent mixing of scalars occurs over a wide range of the Schmidt number ($Sc$), which is the ratio of the kinematic viscosity of the host fluid to the molecular diffusivity of the diffusing scalar. It is well-known that $Sc \ll 1$ for mixing in conducting liquids, $O(1)$ in gaseous-phase mixing and combustion, and $O(10^2 - 10^3)$ for color dyes used in flow visualization experiments and certain biomolecules. The range of scales present in the scalar field is sensitive to $Sc$: for $Sc \lesssim 1$ the smallest scale is estimated to be the Obukhov-Corrsin scale $\eta_{OC} \equiv \eta Sc^{-3/4}$ (where $\eta$ is the Kolmogorov scale) while, for $Sc \gg 1$, the smallest scale is the Batchelor scale $\eta_B \equiv \eta Sc^{-1/2}$. Much attention has been given in the literature to heat transport in air, corresponding to $Sc = O(1)$, and in water, corresponding to $Sc = O(7)$. Accepted results in these instances include a wavenumber spectral roll-off of $k^{-5/3}$ in the inertial-convective range (e.g., [1]), even though deviations from local isotropy and possible intermittency corrections do exist (e.g., [2, 3]). However,

despite the elegant theoretical work of Batchelor [4] and others, the behavior of weakly-diffusive scalars of $Sc \gg 1$ is not as well understood. For instance, Antonia and Orlandi [5] note that there is no consensus yet in the literature concerning Batchelor's [4] $k^{-1}$ spectrum in the viscous-convective range defined by $1/\eta \ll k \ll 1/\eta_B$. Our goal in this paper is to provide some results for the case $Sc \gg 1$.

A major difficulty in studying turbulent mixing at high $Sc$ is the need to resolve scales of size $\eta_B$ which, for $Sc \gg 1$, is much smaller than the smallest scale of the velocity field. This puts stringent demands on the sensor capability in experiments as well as grid resolution and consequent CPU expense in direct numerical simulations (DNS). For the latter case, a relief appears possible because at least some of the essential elements of Batchelor scaling appear to depend only on a large scale-separation between $\eta$ and $\eta_B$, without the requirement of high Reynolds number. Several authors [6–10] have performed simulations for $Sc > 1$ in 3D isotropic turbulence at relatively low Reynolds numbers. In particular, for passive scalars with uniform mean gradients in stationary and forced turbulence, Yeung et al. [8] obtained results for $Sc = 64$ (using a $512^3$ grid) at Taylor-microscale Reynolds number $R_\lambda \approx 38$, while Brethouwer et al. [10] reported limited data at $Sc = 144$ at $R_\lambda \approx 20$. However, even at $Sc = 144$ the scale separation between $\eta$ and $\eta_B$ is only a factor of 12, which is clearly insufficient for convincing demonstrations of scaling properties in the viscous-convection range. (It may be noted that Gotoh et al. [11] studied $Sc = 1000$ at $R_\lambda \approx 3$, but in 2D turbulence.)

In this paper, we present basic results from new simulations for $Sc$ values that are an order of magnitude higher than before; this is made possible by lowering the Reynolds number even further. Specifically we compute mixing for $Sc$ up to 1024 at $R_\lambda \approx 8$ using, as in [8], $512^3$ grid points. Questions may arise, of course, as to whether turbulence at such a low Reynolds number may have "realistic" scaling properties (at least for Kolmogorov's first hypothesis). However, we show (see Section 2) that there is a good collapse of the energy spectrum in Kolmogorov scaling for $R_\lambda$ between 8 and 38. Our primary objective here is to determine, in Section 3, whether inferences based on recent work up to $Sc = 64$ remain valid in the limit of very high $Sc$. These inferences concern, in particular, a sustained trend towards a well-defined Batchelor scaling range in the scalar spectrum, asymptotic approach towards local isotropy, and a saturation of the level of intermittency in single-point statistics of the scalar gradient fluctuations. A summary of this work is given in Section 4.

## 2. Simulation Overview and Resolution Requirements

The numerical algorithms employed are similar to those in our recent work [8]: a Fourier pseudo-spectral method [12] with periodic boundary conditions in space and second-order differences in time is used to solve velocity and scalar transport equations in homogeneous turbulence. Stationary isotropic turbulence is maintained by numerical forcing at the large scales, using the scheme of Eswaran and Pope

[13]. The passive scalar field is generated and maintained stationary by a uniform mean gradient. Velocity and scalar fields in the Fourier space are saved, for further analysis, at time intervals corresponding roughly to one eddy-turnover time. Stationarity in time allows such data sets to be treated as multiple realizations for ensemble averaging. The calculations were carried out on a massively parallel IBM SP computer.

As suggested in Section 1, some care is necessary in choosing the simulation parameters so that the mixing of a passive scalar at $Sc = 1024$ can be simulated with desired accuracy, down to the smallest scales. For the velocity field the commonly applied criterion is that the dimensionless parameter $k_{\max}\eta$ should be at least 1.5, where $k_{\max} = \sqrt{2}N/3$ is the highest wavenumber resolved on an $N^3$ grid. For scalars of $Sc > 1$ the equivalent condition is that $k_{\max}\eta_B = 1.5$ or higher. For $Sc = 1024$ this corresponds to $k_{\max}\eta = 48$, which incidentally provides an opportunity for studying velocity fluctuations in the so-called far-dissipation range of $k\eta \gg 1$ (e.g., [14]).

To obtain a desired value of $k_{\max}\eta$ we note that the Kolmogorov scale $\eta$ depends on the viscosity ($\nu$) and the mean energy dissipation rate ($\langle\epsilon\rangle$), and that in our simulations the latter quantity is largely determined by the forcing parameters. In order to proceed systematically, we retain the same forcing parameters as in the lowest-$R_\lambda$ case in our previous production runs, i.e $R_\lambda \approx 38$ on a $64^3$ grid with $k_{\max}\eta = 1.5$, but increase the viscosity while also refining the grid (with larger $N$ and larger $k_{\max}$). If our new simulation for $Sc = 1024$ is to be carried out on a $512^3$ grid at $k_{\max}\eta = 48$ then the corresponding value of $k_{\max}\eta$ on a $64^3$ grid is 6. The relation $\eta = (\nu^3/\langle\epsilon\rangle)^{1/4}$ suggests that a four-fold increase in $\eta$ can be achieved by increasing the viscosity by a factor of $4^{4/3} = 6.35$. The actual combinations of grid resolution and viscosity used, and the Reynolds and Schmidt numbers attained, are listed in Table I. To give more details on the $Sc$-dependence we have also performed simulations for a range of grid resolutions for intermediate Schmidt numbers. In particular results for $Sc = 64, 128, 256$ on a $256^3$ grid have been averaged over long periods of time.

Although the Reynolds number range simulated in this work obviously falls well below inertial-range requirements, it is important to demonstrate that the

*Table I.* Grid resolution, viscosity, and the Reynolds and Schmidt numbers.

| $N$ | $k_{\max}\eta$ | $\nu$ | $R_\lambda$ | $Sc$ |
|---|---|---|---|---|
| 64 | 1.5 | 0.025 | 38 | 1 |
| 64 | 3 | 0.063 | 20 | – |
| 64 | 6 | 0.159 | 8 | – |
| 128 | 12 | 0.159 | 8 | 1, 4, 8, 16, 32, 64 |
| 256 | 24 | 0.159 | 8 | 64, 128, 256 |
| 512 | 48 | 0.159 | 8 | 256, 512, 1024 |

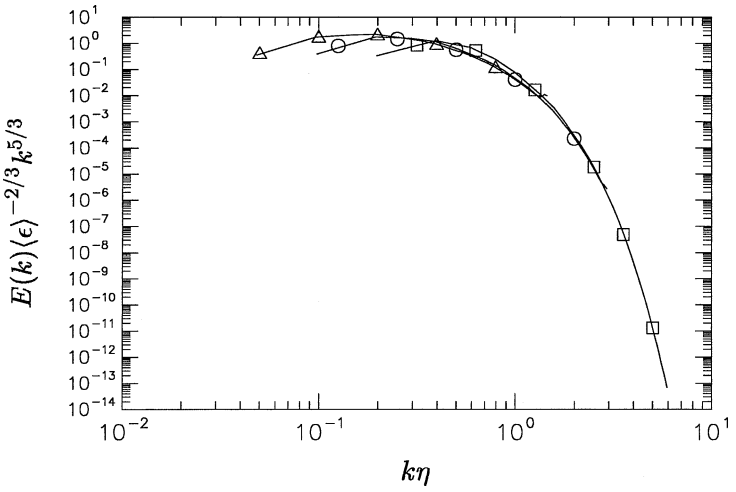


*Figure 1.* Comparison of Kolmogorov-scaled energy spectra at $R_\lambda \approx 38$ (△), 20 (○) and 8 (□), computed on a $64^3$ grid.

small scales in the velocity field still possess the universal behavior associated with Kolmogorov's first hypothesis. Figure 1 shows the 3D energy spectrum function in Kolmogorov variables and at three different Reynolds numbers. It can be seen that, indeed, there is a good collapse of the data, at least for $k\eta > 1$. Because our primary interest is in the viscous-convective range, this result suffices to suggest that the high-$Sc$ behavior driven by the dissipation-range motions in this flow is still physically realistic. On the other hand, when $k\eta$ is extended to very large values, eventually the energy spectrum attains such low values that it becomes contaminated by round-off errors due to finite computer precision. As in [14] use of double-precision arithmetic becomes necessary as far as the far-dissipation range of the velocity field is concerned.

Figure 2 shows a comparison of single versus double-precision results for the energy spectrum, extended to $k\eta = 24$. Because the spectrum is quadratic in the velocity Fourier coefficients, round-off errors in single-precision become dominant at spectral levels of the order $(10^{-8})^2 = 10^{-16}$. It is reasonable to expect round-off error to behave as white noise, which has a flat spectrum, and thus appears with a positive slope because of multiplication by $k^{5/3}$ in the curves shown. It is clear that use of double precision allows the spectrum to be free of contamination by round-off error for spectral levels down to around $O(10^{-33})$ while remaining in good agreement with single precision results before the latter become distorted by round-off.

Because the spectra of high-Schmidt-number scalar fields fall more slowly (as seen later in Figure 4) than does the energy spectrum, the need for double-precision in our passive scalar calculations is less obvious. It is recognized that velocity modes in the far dissipation range contribute little to the spectral cascade of scalars [15], and thus should have little effect on the scalars at the small scales. Numerical tests indeed show only minor differences between results

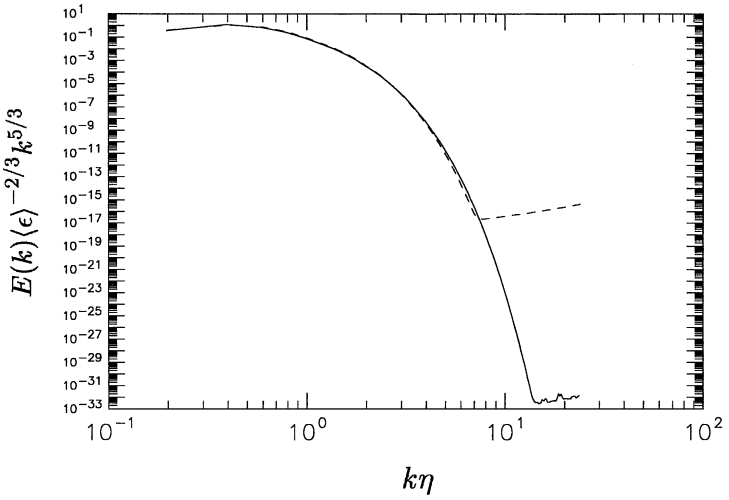


*Figure 2.* Kolmogorov-scaled energy spectra at $R_\lambda \approx 8$ computed on a $256^3$ grid using single-precision (dashed line) and double-precision (solid line) versions of the DNS code.

obtained from single-precision and double-precision codes. Nevertheless, we are motivated by a desire to remove any doubts on the effects of computer precision, and to retain a database useful for future studies of the far-dissipation range of the velocity field. All of the results to follow have been obtained using double-precision versions of our computer codes, at the cost of approximately 50% increase in CPU time mainly due to longer messages in inter-processor communication calls.

## 3. Passive Scalar Results

We are interested in the behavior of scalar fluctuations $\phi$ evolving according to the transport equation

$$\frac{\partial \phi}{\partial t} + u_i \frac{\partial \phi}{\partial x_i} = -u_i \frac{\partial \Phi}{\partial x_i} + D \frac{\partial^2 \phi}{\partial x_i \partial x_i} \tag{1}$$

where $\Phi$ is the mean scalar field, and $D$ is the molecular diffusivity; $u_i$ represents the turbulent velocity field which itself is obtained by solving the Navier–Stokes equations at the specified $R_\lambda$. A basic characterization of the scalar variance and its dissipation rate is first given below, followed by more detailed aspects such as the form of the spectrum and the scaling properties of scalar gradient fluctuations.

### 3.1. Scalar variance and dissipation

The scalar variance $\langle \phi^2 \rangle$ evolves according to

$$\frac{\partial \langle \phi^2 \rangle}{\partial t} = -2\langle u_i \phi \rangle \frac{\partial \Phi}{\partial x_i} - 2D \left\langle \frac{\partial \phi}{\partial x_i} \frac{\partial \phi}{\partial x_i} \right\rangle, \tag{2}$$

where the first term on the right-hand-side is a production term and the second is the mean dissipation rate of scalar variance ($\langle\chi\rangle$). For simplicity we let $\nabla\Phi = (G, 0, 0)$ in Cartesian coordinates, with $G = 1$. Initially $\phi$ is set to be zero everywhere in space. Subsequently both $\langle\phi^2\rangle$ and $\langle\chi\rangle$ are proportional to $G^2$; however, the magnitude of $G$ itself does not appear in the ratio $\langle\phi^2\rangle/\langle\chi\rangle$ (which is the scalar mixing time), nor in appropriately non-dimensionalized quantities.

Although our primary interest is in the stationary state, in Figure 3a and b we show the complete time evolution of the scalar variance and dissipation, for $Sc$ from 64 to 1024 (at $R_\lambda \approx 8$), including data from both the $256^3$ and $512^3$ simulations. (The velocity field statistics in the two simulations are very similar to each other: for instance, their time-averaged energy dissipation rates differ by less than 1%.) Because of the choice of zero initial conditions, at very early times $\phi \approx -u_1 G$,

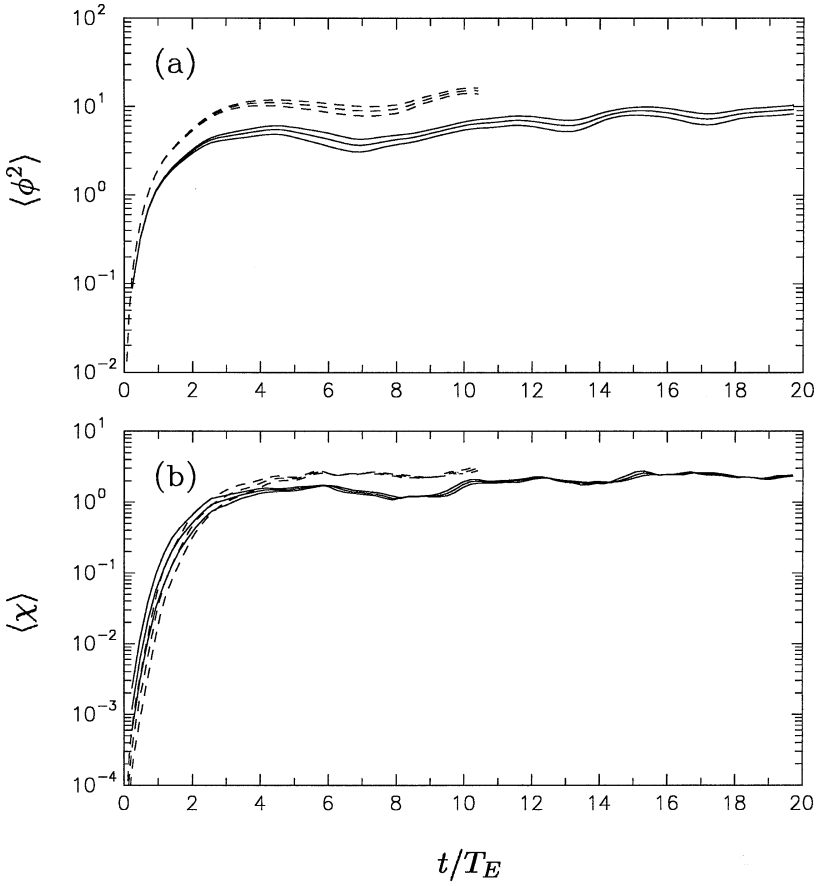


*Figure 3.* Time evolution of (a) scalar variance $\langle\phi^2\rangle$ and (b) scalar dissipation $\langle\chi\rangle$. The time is normalized by the eddy-turnover time $T_E$: data are for $Sc = 64, 128, 256$ on a $256^3$ grid (solid lines), and $Sc = 256, 512, 1024$ on a $512^3$ grid (dashed lines). In (a) the data are monotonically non-decreasing with respect to $Sc$. In (b) they are monotonically non-increasing.

which makes $\langle \phi^2 \rangle$ the same for all scalars whereas $\langle \chi \rangle$ is proportional to the diffusivity $D$. Over time, of course, the properties of each scalar, including its spectrum, adjust to a definite similarity state determined by its Schmidt number. The eventual attainment of stationarity is indicated by the fact that $\langle \chi \rangle$ becomes nearly independent of $Sc$ (thus also demonstrating that the dissipation at small scales is controlled by spectral transfer from the large scales), even though the scalar variance $\langle \phi^2 \rangle$ increases slightly with $Sc$. Together these results imply that the mechanical-to-scalar time scale ratio $r_\phi = (K/\langle \epsilon \rangle)/(\langle \phi^2 \rangle / \langle \chi \rangle)$ decreases slightly with increasing $Sc$, which is consistent with results reported by Yeung and Sawford [16] covering the $Sc$ range from 1/4 to 64.

Substantial "undulations" (more prominent if plotted using linear scales) within the time period of stationarity may be noted in Figure 3(a,b). These are essentially non-ideal features due to the statistical variability in the large-scale motions for which only a limited number of samples can exist in a solution domain of finite size. Stochastic forcing is also known to contribute substantially to the statistical variability over time, which can be minimized only by averaging over long time periods spanning many eddy-turnover times ($T_E$). Our subsequent results are averaged from $t/T_E = 10$ and $t/T_E = 5$ onwards for the $256^3$ and $512^3$ simulations respectively.

### 3.2. Spectra and Batchelor Scaling

A basic feature of increasing Schmidt number in turbulent mixing is a systematic increase of high-wavenumber content in the scalar spectrum, representing fluctuations at increasingly smaller scales. Figure 4 shows these spectra $E_\phi(k)$ in the

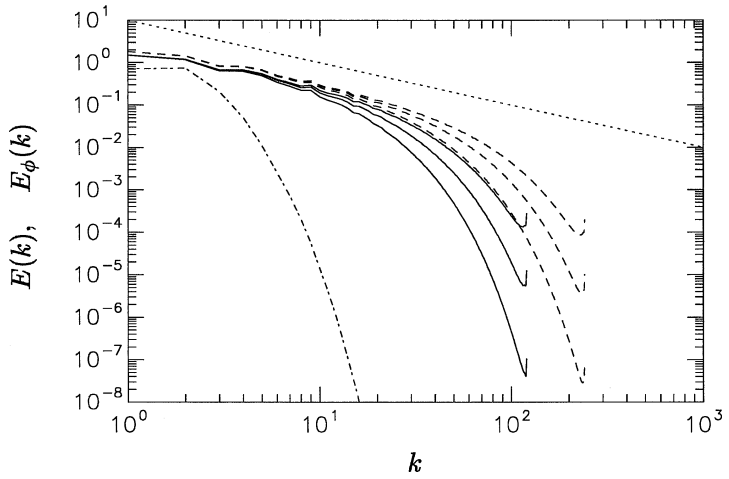


*Figure 4.* Un-normalized 3D spectra for energy and scalars at $R_\lambda \approx 8$: $E(k)$ (chain-dotted line), $E_\phi(k)$ for $Sc = 64, 128, 256$ from $256^3$ simulation (solid lines), and $E_\phi(k)$ for $Sc = 256, 512, 1024$ from $512^3$ simulation (dashed lines). The dotted line shows slope $-1$ for reference.

range $Sc = 64$ to 1024, as well as the energy spectrum $E(k)$. It is well known (see, e.g., [17, 18]) that, even for $Sc = 1$, the scalar spectrum falls off more slowly with wavenumber than the classical $-5/3$ slope, because a remnant of the $k^{-1}$ region appears already. The present data at high $Sc$ are well above the round-off levels suggested in Figure 2. The spectra for $Sc = 256$ computed from $256^3$ and $512^3$ simulations are seen to virtually coincide, which suggests $k_{\max}\eta_B = 1.5$ gives sufficient resolution, at least for second-order statistics. Furthermore, as $Sc$ increases, the spectral form appears to gain closer resemblance to $k^{-1}$ behavior in an intermediate range of scales.

A primary motivation for simulating $Sc = O(10^3)$ is the expectation of a sufficiently wide scaling range between $\eta$ and $\eta_B = \eta Sc^{-1/2}$, so that the status of $k^{-1}$ Batchelor scaling in the viscous-convective range can be resolved. Both Batchelor's [4] original result (assuming quasi-steady strain rates of order $(\langle\epsilon\rangle/\nu)^{1/2}$), namely,

$$E_\phi(k) = q\langle\chi\rangle(\nu/\langle\epsilon\rangle)^{1/2}k^{-1}\exp(-q(k\eta_B)^2), \tag{3}$$

where $q$ is a dimensionless coefficient known as Batchelor constant in the high $Sc$ limit, and Kraichnan's [19] modification of it (accounting for rapid fluctuations of the strain-rate), namely,

$$E_\phi(k) = q\langle\chi\rangle(\nu/\langle\epsilon\rangle)^{1/2}k^{-1}(1 + (6q)^{1/2}k\eta_B)\exp(-(6q)^{1/2}(k\eta_B)), \tag{4}$$

are well-known, reducing to $E_\phi(k) = q\langle\chi\rangle(\nu/\langle\epsilon\rangle)^{1/2}k^{-1}$ in the range $k\eta_B \ll 1$. In addition, to facilitate comparison with experiment we also consider corresponding scaling behavior in the 1D spectrum $E_{1\phi}(k_1)$, where $k_1$ is a single Cartesian wavenumber component. If the scalar field is isotropic (or nearly so), $E_{1\phi}(k_1)$ can be obtained by averaging over the three coordinate axes, or derived from the 3D spectrum $E_\phi(k)$ by the isotropy relation [20] $E_{1\phi}(k) = -\int_k^\infty E_\phi(k)/k\,dk$ (see also [6]).

In Figure 5 we show both the three- and 1D spectra in normalized form, for scalars with Schmidt numbers ranging from 64 to 1024. The data support a $k^{-1}$ scaling range, especially in the 3D spectrum on log-log scales for $k\eta_B$ roughly between 0.02 and 0.08, although the attainment of a true plateau appears less definite under a stricter test posed by the use of log-linear scales (see insets). Our data also show, despite some small differences in the viscous-diffusive range ($k\eta > 1$), an excellent degree of agreement with Kraichnan's expression, and slower decay at high wavenumbers than suggested by Batchelor. The coefficient $q$ depends weakly on $Sc$ for $Sc < 64$, as already noted in [8]. Nevertheless, our present result at higher Schmidt numbers also suggest an asymptotic value between 5 and 6, which is in good agreement with deductions based on a study of structure functions in physical space [22].

Although classical arguments suggest that the width of an apparent $k^{-1}$ scaling range (as seen above) is primarily contingent upon having a sufficiently high Schmidt number, it is of interest to ascertain whether there is also a Reynolds number dependence. To address this question we compare in Figure 6 normalized spectra for three Reynolds and Schmidt number combinations, using in part data

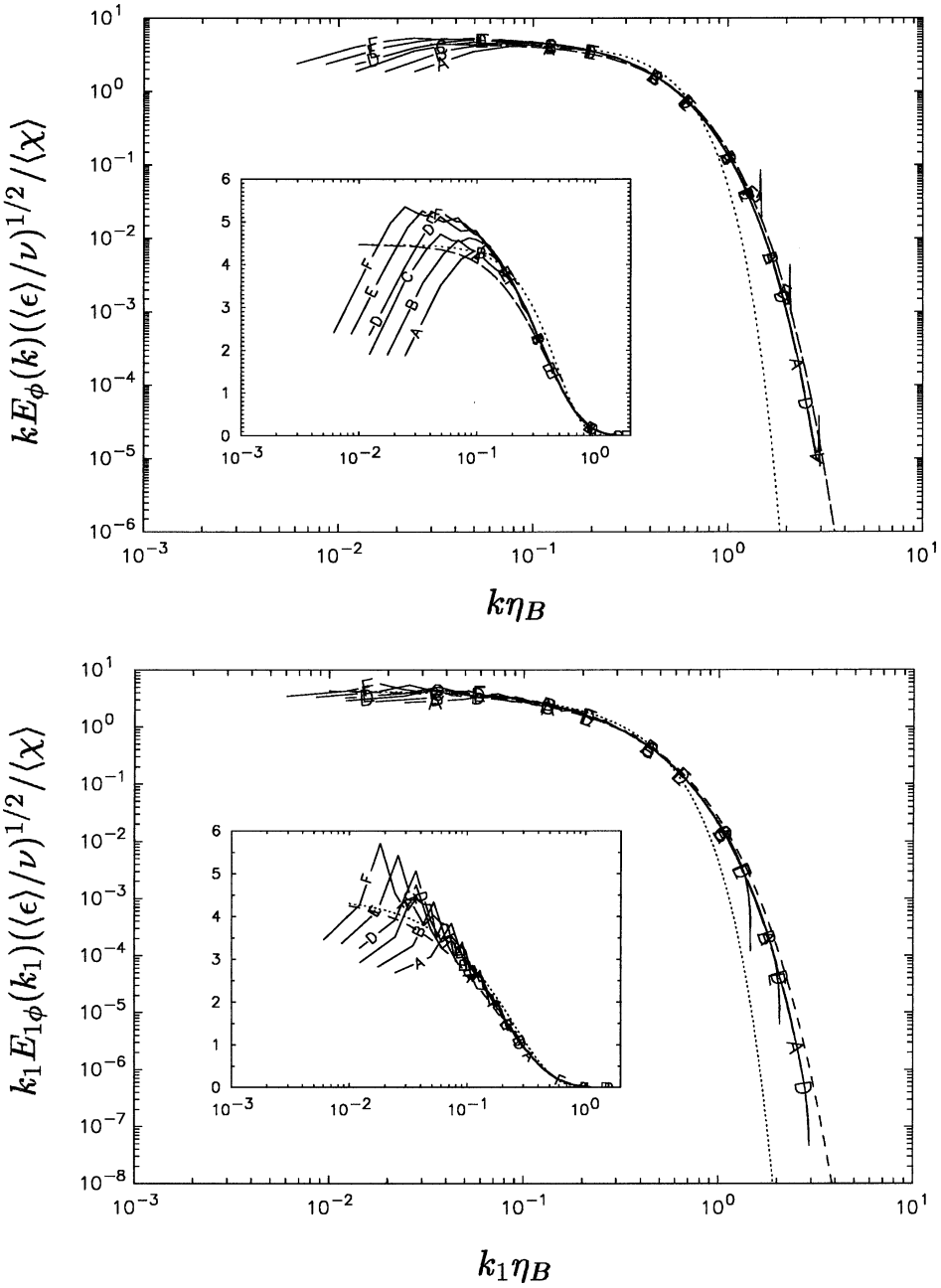


*Figure 5.* The scalar spectrum in 3D (top) and 1D (bottom) versions scaled by Batchelor variables for high-Schmidt-number scalars at $R_\lambda \approx 8$: $Sc = 64, 128, 256$ (A-C) from $256^3$ simulation, and $Sc = 256, 512, 1024$ (D-F) from $512^3$. The data are compared with Batchelor's (dotted line) and Kraichnan's (dashed line) expressions calculated with $q = 2\sqrt{5}$ which is based on a theoretical estimate by Qian [21].

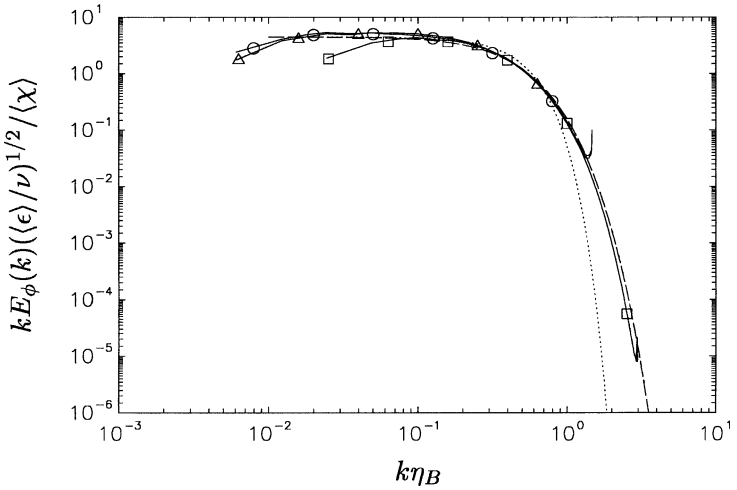


*Figure 6.* 3D scalar spectrum normalized by Batchelor variables, for the cases ($R_\lambda$ 38, $Sc = 64$: △), ($R_\lambda$ 8, $Sc = 64$; □), and ($R_\lambda$ 8, $Sc = 1024$: ○). Dotted and dashed lines represent Batchelor and Kraichnan formulas as in Figure 5.

from Yeung et al. [8] for $R_\lambda \approx 38$. An increase of $Sc$ from 64 to 1024 with $R_\lambda$ held constant (at 8) produces, as expected, results closer to $k^{-1}$ scaling with a wider range. However, a similar effect can also be observed when $R_\lambda$ is increased (from 8 to 38) while $Sc$ is held constant (at 64). These results suggest that the actual requirement for high $Sc$ may be weakened (say, towards only moderately large values) if the Reynolds number is high. We shall return to this issue in the context of other results in this paper.

### 3.3. Scalar gradients, local isotropy and intermittency

For many reasons (e.g., see [23]), the small-scale structure of velocity and scalar fluctuations in turbulence is important in both practical applications and theoretical development. Two of the essential elements of classical Kolmogorov phenomenology are that, at high Reynolds numbers, the small scales of turbulence become locally isotropic, and also increasingly intermittent via the occurrence of intense and localized fluctuations. However, a large body of evidence from both experiments and simulations (see [2, 3] for a summary) have clearly indicated that, at least for scalars with $Sc = O(1)$, first-order departures from local isotropy may persist even to very high Reynolds number. Furthermore, various measures such as derivative flatness factors and intermittency exponents inferred from two-point correlators indicate that the scalar field is generally more intermittent than the velocity field. An important question, which has not been addressed in the usual phenomenology, is the possible dependence of these statistics on the Schmidt number, especially when $Sc$ is large and the scalar fluctuations become strongly influenced by the strain-rate fluctuations in the velocity field.

In a recent paper [8] we studied the issue of local isotropy via the skewness of scalar gradient fluctuations $\nabla_\parallel \phi$ parallel to the imposed mean scalar gradient: this skewness decreased systematically as the $Sc$ was varied from 1/4 to 64 (roughly by powers of 2), with $R_\lambda$ held constant at about 38. Data from Yeung et al. [8] and the present simulations at $R_\lambda \approx 8$ are shown together in Figure 7. It is clear, again, that there is a systematic decrease of the skewness at high $Sc$, with perhaps both datasets following power-law scaling for $Sc > O(10)$. Careful comparison of data for $R_\lambda$ of 38 and 8 does reveal, however, some modest differences which imply that there are some Reynolds number effects which remain to be understood.

Another conclusion from Yeung et al. [8] is that the scalar gradient fluctuations become more intermittent with increasing $Sc$, but most likely approach a saturated asymptotic level in the high-$Sc$ limit. The present data at $R_\lambda$ of 8 are shown in Table II. Comparisons between data sets at the same $Sc$ but different grid resolution suggest that an effect of marginal grid resolution for a given $Sc$ is a slight underestimate for the flatness factor. (This effect may, however, be obscured by the fact that higher-resolution simulations are generally run over a shorter period of time and thus may be more prone to statistical variability.) Nevertheless, we can conclude that the flatness of $\nabla_\parallel \phi$ (parallel to the mean gradient) does not increase further with $Sc$ when the latter is beyond (roughly) 64, followed by the same behavior of $\nabla_\perp \phi$ (perpendicular to the mean gradient) for $Sc$ around 256. The asymptotic flatness level attained is about 10, which is somewhat lower than about 12 at $R_\lambda \approx 38$ in Yeung et al. [8]. The increasing closeness, with increasing $Sc$, between the

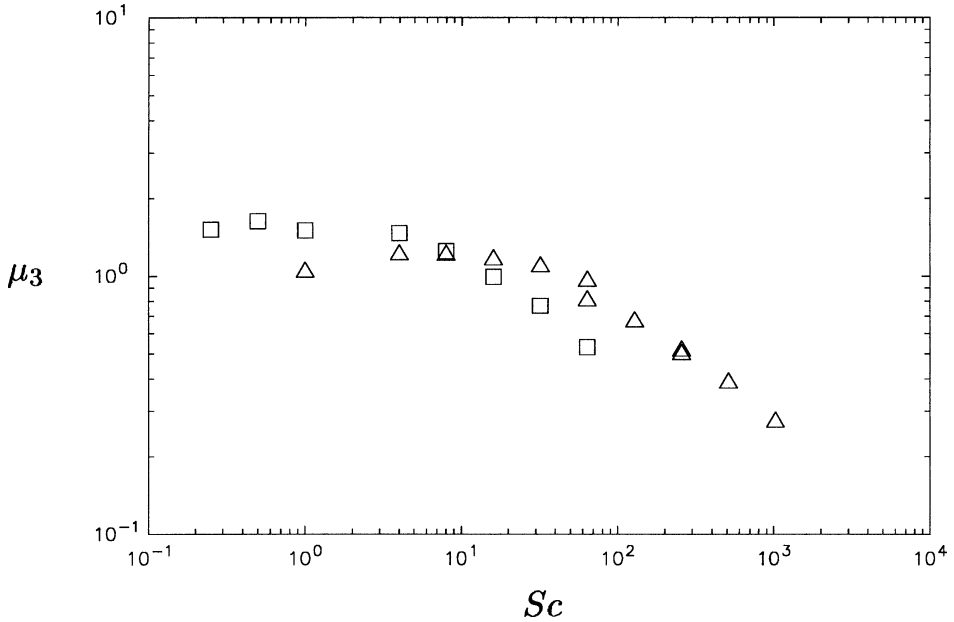


*Figure 7.* Skewness factor ($\mu_3$) of $\nabla_\parallel \phi$ versus Schmidt number, at $R_\lambda$ of 8 (△) and 38 (□, from [8]).

*Table II.* Flatness factors, $\mu_4$, of the scalar gradient components, in directions parallel and perpendicular to the mean gradient, from simulations at $R_\lambda \approx 8$.

| $Sc$ | Grid | $k_{\max}\eta_B$ | $\mu_4(\nabla_\parallel \phi)$ | $\mu_4(\nabla_\perp \phi)$ |
|---|---|---|---|---|
| 1 | $128^3$ | 11.9 | $5.2 \pm 1.02$ | $4.6 \pm 0.57$ |
| 4 | $128^3$ | 6.0 | $7.1 \pm 1.55$ | $6.4 \pm 0.87$ |
| 8 | $128^3$ | 4.2 | $7.8 \pm 1.56$ | $7.2 \pm 0.93$ |
| 16 | $128^3$ | 3.0 | $8.4 \pm 1.54$ | $7.8 \pm 0.96$ |
| 32 | $128^3$ | 2.1 | $8.9 \pm 1.46$ | $8.3 \pm 0.97$ |
| 64 | $128^3$ | 1.5 | $8.8 \pm 1.22$ | $8.4 \pm 0.84$ |
| 64 | $256^3$ | 3.0 | $8.8 \pm 1.45$ | $8.8 \pm 0.96$ |
| 128 | $256^3$ | 2.1 | $9.1 \pm 1.29$ | $8.9 \pm 0.94$ |
| 256 | $256^3$ | 1.5 | $9.0 \pm 1.05$ | $8.7 \pm 0.78$ |
| 256 | $512^3$ | 3.0 | $9.9 \pm 1.40$ | $9.8 \pm 1.47$ |
| 512 | $512^3$ | 2.1 | $10.2 \pm 1.18$ | $10.1 \pm 1.68$ |
| 1024 | $512^3$ | 1.5 | $9.9 \pm 0.89$ | $10.0 \pm 1.82$ |

flatnesses of $\nabla_\parallel \phi$ and $\nabla_\perp \phi$ is consistent with the reduction of small-scale anisotropy of the small-scale scalar. The requirement of a higher $Sc$ (64 in the present case, compared with $O(4)$ in Yeung et al. [8]) for the attainment of the asymptotic behavior is also consistent with trends noted in the skewness data in Figure 7 as well as the spectra shown in Figure 6. In other words, the asymptotic state of the scalar seems to require a higher value of $Sc$ when $R_\lambda$ becomes smaller.

Finally, we show in Figure 8 the probability density function (PDF) of $\nabla_\parallel \phi$ at the same $Sc$ as in Table II. The most significant Schmidt number effects are in the range 1–64 (lines A–C), where the left half (for $\nabla_\parallel \phi < 0$) becomes stretched out, leading to the reduced skewness seen in Figure 7. With further increase in $Sc$, the widths of the tails on both sides change very little, consistent with the gradient flatness approaching an asymptotic level as suggested by the numbers in Table II. The asymptotic shape of this PDF is apparently close to a stretched-exponential.

## 4. Discussion and Conclusions

In order to help resolve several important issues concerning the scaling of weakly diffusive passive scalars in 3D turbulent mixing, we have performed a series of direct numerical simulations (DNS) aimed at reaching Schmidt numbers ($Sc$) an order of magnitude higher (we believe) than has been attained previously for 3D turbulent mixing. Specifically, we have reached $Sc = 1024$ based on a simulation using $512^3$ grid points. Satisfactory resolution of scalar fluctuations at the Batchelor scale is maintained by reducing the Reynolds number to a value of 8 (when based on the Taylor microscale). Care is taken to verify that the small-scale motions in

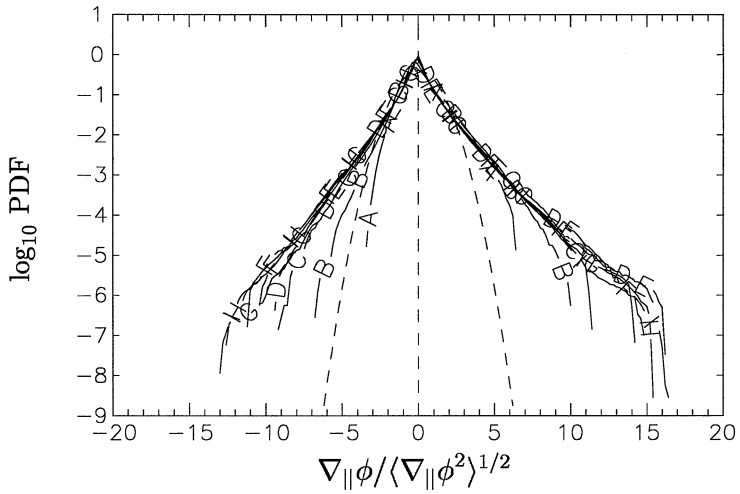


*Figure 8.* Logarithm (to base 10) of the standardized PDF of $\nabla_{\|}\phi$ for at different Schmidt numbers: 1,8,64 (A–C, from $128^3$ simulation), 64,128,256 (D–F, from $256^3$), and 256, 512, 1024 (G–I, from $512^3$). For comparison the dashed curve shows the standard Gaussian distribution.

the velocity field at this Reynolds number satisfy the classical dissipative-scale universality to a reasonable degree, and that the energy spectrum in the far-dissipation range is not contaminated by round-off errors due to the finite precision of computer arithmetic. We emphasize that the attainment of a well-defined viscous-convective range requires (very) high Schmidt number, but not high Reynolds number.

Our focus in data analysis has included the behavior of scalar variance and dissipation rate, the spectral shape in respect of the classical Batchelor $k^{-1}$ scaling, and the statistics of passive gradients bearing upon the central issues of local isotropy and intermittency. Passive scalar fluctuations are generated and maintained by a uniform mean gradient within forced isotropic turbulence, and statistics are collected over an extended period of stationarity in time. Consistent with previous results, the scalar fluctuations attain a self-similar state where the variance increases slightly with $Sc$, but the dissipation rate is essentially independent of $Sc$. The scalar spectrum increasingly resembles the $k^{-1}$ viscous-convective range as $Sc$ is raised systematically from 64 to 1024 in powers of 2, and the Kraichnan [19] form continues to be a very good approximation in the viscous-diffusive range. Scalar gradient statistics computed for $R_\lambda \approx 8$ confirm the trend of reduced skewness and approach to local isotropy in the high-$Sc$ limit. However, the value or range of $Sc$ for peak skewness at $R_\lambda$ of 8 appears to be somewhat higher when compared with previous results at $R_\lambda$ of 38. The level of intermittency manifested in single-point scalar gradient flatness factors shows the same trend as in Yeung et al. [8], namely a saturation at high $Sc$. This saturation now requires at $R_\lambda$ 8 a minimum of $Sc \approx 64$. It thus appears that increasing $Sc$ at the cost of decreasing $R_\lambda$ has some limitations, and there may be physical features whose understanding requires both large $R_\lambda$ and large $Sc$. For other features such as the probability distribution of scalar gradient

fluctuations, which continues to be close to a stretched-exponential, the precise value of $R_\lambda$ does not seem to be important.

To summarize, we have documented the basic results from numerical simulations of 3D turbulent mixing at very high Schmidt number, and have used data over an extended range of Schmidt numbers (1–1024) to address several important issues in Schmidt-number-scaling of passive scalar fluctuations driven by a uniform mean gradient. This new database is expected to be useful for further studies of more detailed aspects of passive scalar mixing, such as the behavior of spatial structure represented by intermittency in two-point correlators, fluctuations of the scalar dissipation rate, and multifractal statistics. These will be reported elsewhere.

## Acknowledgments

The authors gratefully acknowledge support from the National Science Foundation, via Grants CTS-0121030 (PKY) and CTS-0121007 (KRS), as well as via NSF cooperative agreement ACI-9619020 through computing resources provided by the National Partnership for Advanced Computational Infrastructure at the San Diego Supercomputer Center. Our thanks go to Dr. Joerg Schumacher for a helpful discussion at the time of planning the simulations.

It is a pleasure to dedicate this paper to Prof. Robert A. Antonia on the occasion of his 60th birthday.

## References

1. Sreenivasan, K.R., The passive scalar spectrum and the Obukhov-Corrsin constant. *Phys. Fluids* **8** (1996) 189–196.
2. Sreenivasan, K.R., On local isotropy of passive scalars in turbulent shear flows, In: *Proceedings of the Royal Society of London*, Vol. 434 (1991) pp. 165–182.
3. Warhaft, Z., Passive scalars in turbulent flows. *Ann. Rev. Fluid Mech.* **32** (2000) 203–240.
4. Batchelor, G.K., Small-scale variation of convected quantities like temperature in turbulent fluid. *J. Fluid Mech.* **5** (1959) 113–133.
5. Antonia, R.A. and Orlandi, P., Effect of Schmidt number on passive scalar turbulence. *Appl. Mech. Rev.* **56** (2003) 615–632 .
6. Bogucki, D., Domaradzki, J.A. and Yeung, P.K., Direct numerical simulations of passive scalars with $Pr > 1$ advected by turbulent flow. *J. Fluid Mech.*, **343** (1997) 111–130.
7. Yeung, P.K., Sykes, M.C. and Vedula, P., Direct numerical simulation of differential diffusion with Schmidt numbers up to 4.0. *Phys. Fluids* **12** (2000) 1601–1604.
8. Yeung, P.K., Xu S. and Sreenivasan, K.R., Schmidt number effects on turbulent transport with uniform mean scalar gradient. *Phys. Fluids* **14** (2002) 4178–4191.
9. Orlandi, P. and Antonia, R.A., Dependence of the nonstationary form of Yaglom's equation on the Schmidt number. *J. Fluid Mech.* **451** (2002) 99–108.
10. Brethouwer, G., Hunt, J.C.R. and Nieuwstadt, F.T.M., Micro-structure and Lagrangian statistics of the scalar field with a mean gradient in isotropic turbulence. *J. Fluid Mech.* **474** (2003) 193–225.
11. Gotoh, T., Nagaki, J. and Kaneda, Y., Passive-scalar spectrum in viscous-convective range in two-dimensional turbulence. *Phys. Fluids* **12** (2000) 155–168.

12. Rogallo, R.S., Numerical experiments in homogeneous turbulence. NASA Tech. Memo. 81315, NASA Ames Research Center (1981).
13. Eswaran, V. and Pope, S.B., An examination of forcing in direct numerical simulations of turbulence. *Comput. Fluids* **16** (1988) 257–258.
14. Chen, S., Doolen, G., Herring, J.R. and Kraichnan, R.H., Far-dissipation range of turbulence. *Phys. Rev. Lett.* **70** (1993) 3051–3054.
15. Yeung, P.K., Multi-scalar triadic interactions in differential diffusion with and without mean scalar gradients. *J. Fluid Mech.* **321** (1996) 235–278.
16. Yeung, P.K. and Sawford, B.L., Random sweeping hypothesis for passive scalars in isotropic turbulence. *J. Fluid Mech.* **459** (2002) 129–138.
17. Yeung, P.K. and Pope, S.B., Differential diffusion of passive scalars in isotropic turbulence. *Phys. of Fluids A* **5** (1993) 2467–2478.
18. Mydlarski, L. and Warhaft, Z., Passive scalar statistics in high-Péclet-number grid turbulence. *J. Fluid Mech.* **358** (1998) 135–175.
19. Kraichnan, R.H., Small-scale structure of a scalar field convected by turbulence. *Phys. Fluids* **11** (1968) 945–953.
20. Monin, A.S. and Yaglom, A.M., *Statistical Fluid Mechanics.* Vol. II. MIT Press, Cambridge, MA (1975).
21. Qian, J., Viscous range of turbulent scalar of large Prandtl number. *Fluid Dynam. Res.* **15** (1995) 103–112.
22. Borgas, M.S., Sawford, B.L., Xu, S., Donzis, D.A. and Yeung, P.K., High Schmidt number scalars in turbulence: structure functions and Lagrangian theory. *Phys. Fluids* (2003) Submitted.
23. Sreenivasan, K.R. and Antonia, R.A., The phenomenology of small-scale turbulence. *Ann. Rev. Fluid Mech.* **29** (1997) 435–472.